JOURNAL OF APPLIED ELECTROCHEMISTRY 25 (1995) 933–939

Jet electrochemical etching of nickel in a sodium chloride medium assisted by a pulsed laser beam

V. LESCURAS, J. C. ANDRÉ, F. LAPICQUE

Laboratoire des Sciences du Génie Chimique and Département de Chimie Physique des Réactions, CNRS–ENSIC, 1 rue Grandville, BP 451, F-54001 Nancy, France

I. ZOUARI

Ecole Nationale d'Ingénieurs de Gabès, Département de Génie Chimique, Route de Medenine, 6029 Gabès, Tunisia

Received 11 January 1995; revised 6 April 1995

This paper deals with the jet electrochemical etching of metal, using nickel drilling as an example; the performance of this technique was investigated as a function of the nozzle diameter and current density. The significance of the outer dissolution of metal, due to liquid spreading on the vertical substrate facing the nozzle, was estimated; the hole size was compared to the nozzle diameter. Moreover, a pulsed beam was shown to improve the precision of the edge. Applications to shape patterning are presented and discussed.

1. Introduction

In recent years, processes for the manufacture of small-size objects have been investigated and improved for various applications in electronics, mechanics, aeronautics and, more recently, in the area of sensors and actuators. Small-size objects can be produced either by deposition, etching, or both, using chemical or electrochemical methods, in mask or maskless operations, and with the possible assistance of an incident beam. As regards etching, the mechanical precision of the pieces depends on the nature of the fluid phase, the flow conditions and the wavelength of the incident beam, generated by lasers or X-ray synchrotrons.

The application of etching processes is governed by the mechanical precision and therefore by the technique used. The various available techniques and, in particular, the electrochemical processes, have been reviewed by Datta and Romankiw in 1989 [1]. In general, the rate of metal electrodissolution, proportional to the current density, depends on the local hydrodynamics and the applied potential. Moreover, the use of passivating electrolytes under transpassivating conditions yields etched profiles of higher precision than non-passivating solutions [2, 3].

Numerous processes rely on the use of a mask for the local irradiation of a polymeric layer, prior to chemical or electrochemical operations [4–6]. Better than micrometre accuracy can be obtained over the height of the structure and these promising techniques are adapted for manufacturing of sensors and actuators and for their integration into microsystems, in spite of the heavy equipment required for large-scale production.

Electrochemical machining (ECM) can be operated with fair etching rates and without a mask [7, 8]. The mechanical precision is of the order of a fraction of a millimetre. However, the current density is limited by the removal of heat and the production of gas, which may result in drastic sparking phenomena [9, 10]; in addition, dissolution occurs on the whole active metal surface. Jet techniques have been proposed to avoid this latter drawback, and the turbulence extent at the impinged surface results in high-speed electrochemical deposition or etching [1]. Jet plating technology involves precious metals but also copper, tin, zinc or alloys, and could be used for the production of printed circuit boards [11]. Nevertheless, the main application of jet electrochemical processes probably concerns small-size mechanics and prototyping. The incident beam of a continuous Ar laser, was shown to improve the deposition yield and the properties of the metal deposited [12–14] with a jet device. More recently, the jet electrodeposition of zinc was investigated by our group [15, 16] and the assistance of a colinear pulsed laser beam was reported to improve the metal morphology by an appreciable grain coalescence and a reduction in grain size.

The aim of this paper is to highlight the electrochemical etching of metal in a nonpassivating medium with assistance of a pulsed laser beam: nickel dissolution in a sodium chloride solution, has been carried out. In particular, the limits of the technique are investigated in terms of drilling efficiency, mechanical precision of the etching operation and metal morphology. For this purpose, systematic study of hole drilling is first conducted using nozzles of various diameters; then, the capacity and the limits of the jet etching technique are followed through machining trials on nickel objects.

0021-891X

2. Experimental details

2.1. *Experimental device*

The experimental setup depicted in Fig. 1 is similar to that previously used for zinc deposition [16]. The electrolytic cell was machined out of Altuglas™ (methyl polymethacrylate) and consisted of an inlet chamber, a nozzle and a substrate support facing the nozzle section. A platinum sheet placed in the chamber acted as the cathode. The laser source was a YAG pulsed laser at 532 nm with a repetition rate of 30 Hz. The laser beam entered colinear to the liquid jet, which allowed the closure of the electrical circuit and acted as a waveguide. The average incident power, when used, was fixed at 1 W. The anode was a 150 μm thick plate of 99% nickel; the piece was attached to a computer-controlled X–Z table, allowing displacements in a vertical plane (Fig. 1). The computer was also used to synchronize the gate-on of the laser beam with the closure of the electrical circuit.

Two types of nozzles were used as shown in Fig. 2(a) and (b). First, conical nozzles were machined out of Altuglas™; however, these pieces could not be drilled below 200 μm by conventional tools. Smaller jet sizes could be considered using silicon nozzles. Square holes were machined out of silicon by the Laboratoire de Physique et Métrologie des Oscillateurs, Besançon, France, using aqueous solutions of ethylenediamine and pyrocatechol; silicon was thus machined along the (1 0 0) plane of the Si structure allowing a precision of one micrometre to be obtained. The machined pieces (10 mm × 10 mm)

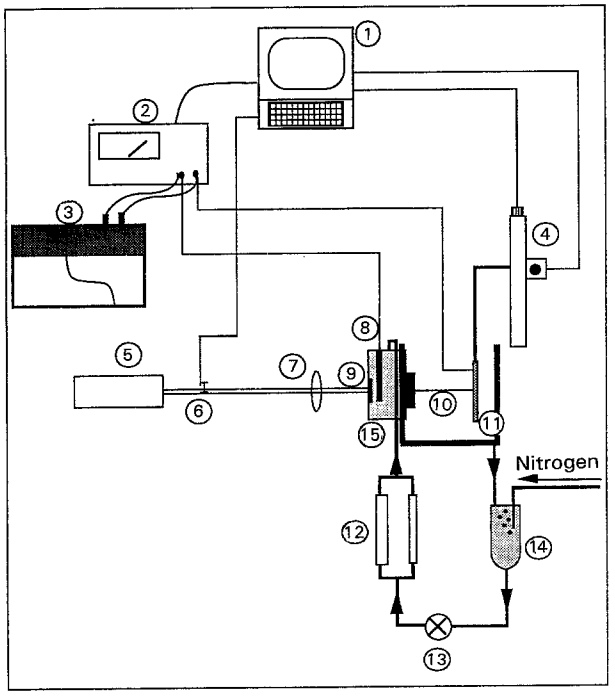

Fig. 1. Scheme of the experimental setup: (1) computer, (2) potensiostat, (3) recorder, (4) step-by-step motors, (5) YAG pulsed laser (532 nm), (6) shutter, (7) convergent lens, (8) counter-electrode, (9) Window (BK7™), (10) nozzle, (11) working electrode, (12) flow meters, (13) gear pump, (14) reservoir and (15) inlet chamber.

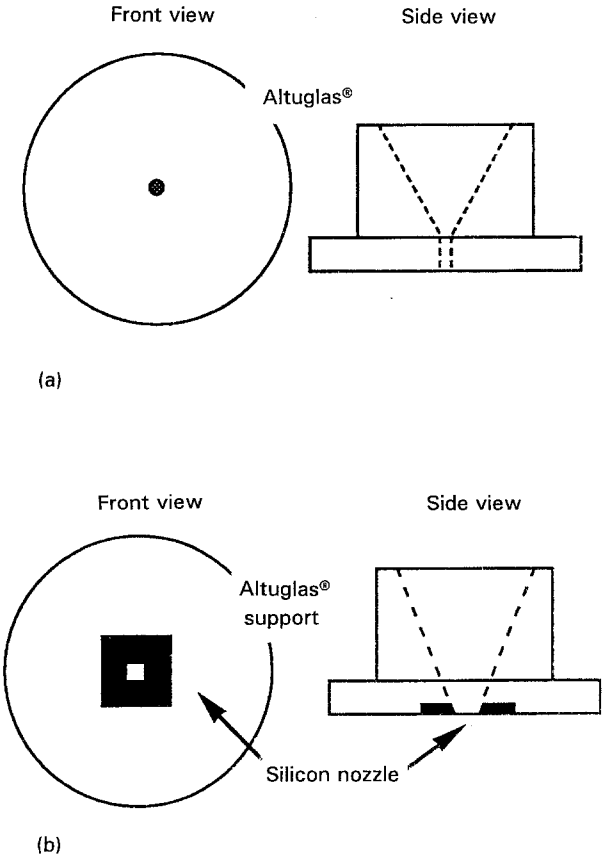

Fig. 2. Schematic view of the nozzle: (a) Altuglas™ nozzle and (b) silicon piece mounted onto the Altuglas™ nozzle.

were glued onto the polymeric pieces which acted as supports in this case. Both types of nozzle were observed using a binocular viewer, allowing the quality of the nozzle outlet to be controlled. Moreover, the nozzle size was measured by SEM observations.

2.2. *Chemical system*

The electrolyte solution was a 5 M sodium chloride medium. The sodium salt was of analytical grade (Prolabo, France). The viscosity of the solution, measured using a Ubbelohde device, was 1.58×10^{-6} $m^2 s^{-1}$ at 20 °C. The electrical conductivity of the solution was measured at 22 $\Omega^{-1} m^{-1}$ at this temperature.

3. Investigation of nickel drilling

3.1. *Experimental conditions*

A systematic investigation of metal drilling was first conducted to define the capacities and the limits of electrochemical drilling in a nonpassivating medium; in particular, the etching rate, the efficiency and the geometrical qualities of the etched holes were investigated under several operating conditions. All experiments were carried out at ambient temperature which ranged from 19 to 22 °C.

The applied cell voltage was in the range 5 to 40 V: the major part of the voltage corresponded to the ohmic drop in the jet. The nozzle diameter, d, was varied from 125 to 531 μm. The velocity of the

electrolyte solution was maintained between 8 and 11 m s^{-1}. Previous investigations [16], together with experimental observations, showed that continuous liquid jets could be produced with this velocity range. The distance between the nozzle outlet and the nickel substrate was positioned at from 6 to 10 times the nozzle diameter; this distance corresponds to the zone of a well-established regime for a free jet in turbulent flow in which both the jet diameter and the velocity can be considered as constant [17]. The substrate, mounted on the extension arm, was displaced on the axis of the liquid jet by means of a micrometric device and the distance was measured by optical observations. The gap had to be larger than one millimetre to avoid the formation by capillary forces of a liquid drop between the nozzle outlet and the nickel plate, and a resulting electrical short circuit. This phenomenon might represent an additional limit in the minimum dimensions of jet electrochemical devices.

3.2. *General features of electrochemical drilling*

For most runs, the current recorded at imposed cell voltage remained fairly constant. The perforation of the nickel plate was observed as the liquid solution flowed on its rear face: this was related to a sudden change in the current. The shape of the hole was then roughly conical. Maintaining the cell voltage allowed metal dissolution to occur, resulting in the formation of a cylindrical hole. The time required for machining the hole, of conical or cylindrical shape, Δt, was recorded. The current was averaged over this period. The current density, i, was defined as the ratio of the time-averaged current to the cross-section of the nozzle. For a given cell voltage, i was a decreasing function of the nozzle diameter, due to the importance of ohmic drop in the jet; hence, parameters i and d are not totally independent.

The shape and the hole dimensions were observed with binocular viewer and SEM observations. As shown in Fig. 3 several zones of the drilled metal surface can be defined. First, the impact zone surrounding the hole corresponds to the wall surface of the hole: this zone cannot be observed from a top view for perfectly cylindrical holes. Two zones of less significant etching are also observed: a peripheral zone, with a diameter much larger than the nozzle diameter, due to the spreading of the jet at the vertical surface, and the so-called ring zone, a transition region between the peripheral zone and the walls of the hole.

The hole diameters at the front and the rear sides of the nickel plates, d_f and d_r, respectively, were generally larger than the nozzle diameter, d. The holes were considered to be of cylindrical geometry when the rear diameter, d_r, differed from d_h by less than 5%. Otherwise, conical geometry was assumed and the volume, V, of the hole was calculated taking into account the plate thickness, e, and the diameters d_f and d_r.

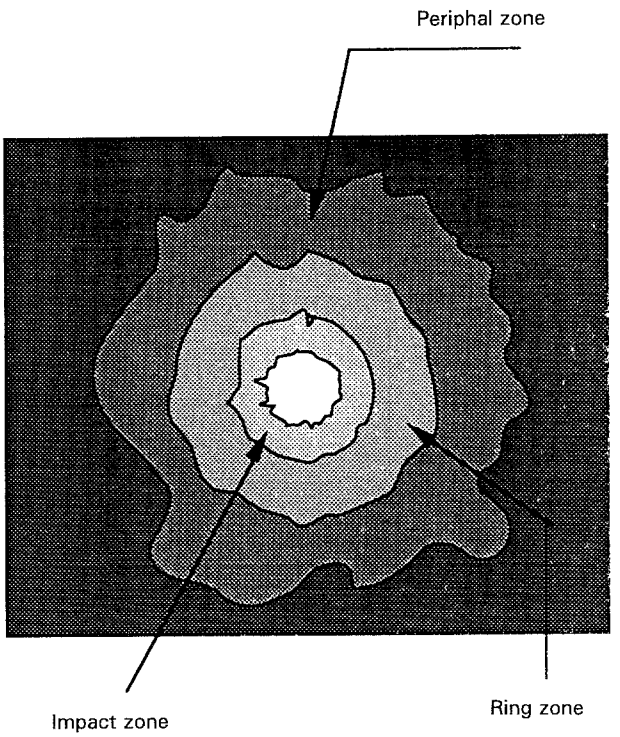

Fig. 3. View of a hole drilled in the nickel sheet.

3.3. *Etching rate and efficiency*

The etching rate was defined as the ratio of the plate thickness to the time required for the drilling operation. The theoretical etching rate was calculated by Faraday's law. Figure 4(a) and (b) establish the comparison of the two etching rates. Whereas the theoretical rate increased linearly with i, as expected, the experimental rate was hardly affected by a rise in current density: after a slight increase at low current densities, the rate levelled off and remained below 1 μm s^{-1}, for both hole shapes. The influence of the nozzle diameter was of negligible effect, and the incident beam did not result in a significant increase, as observed for zinc deposition [16].

Measurements of weight losses of the machined nickel plates revealed that the faradaic yield of the dissolution was close to unity within 10%, for all conditions of current density and nozzle diameter. Therefore, it can be deduced that the large difference between the two etching rates was due to dissolution phenomena, which were not taken into account in the theory:

(i) the etching operation resulted in holes with diameters d_f and d_r, larger than the nozzle diameters, in accordance with observations of the samples;
(ii) the existence of the two external zones shown in Fig. 3 corresponded to additional electrical charge spent for metal dissolution.

To separate the effects of phenomena (i) and (ii), the etching efficiency, Φ, was introduced as the ratio of the charge required for the dissolution of the volume V, to

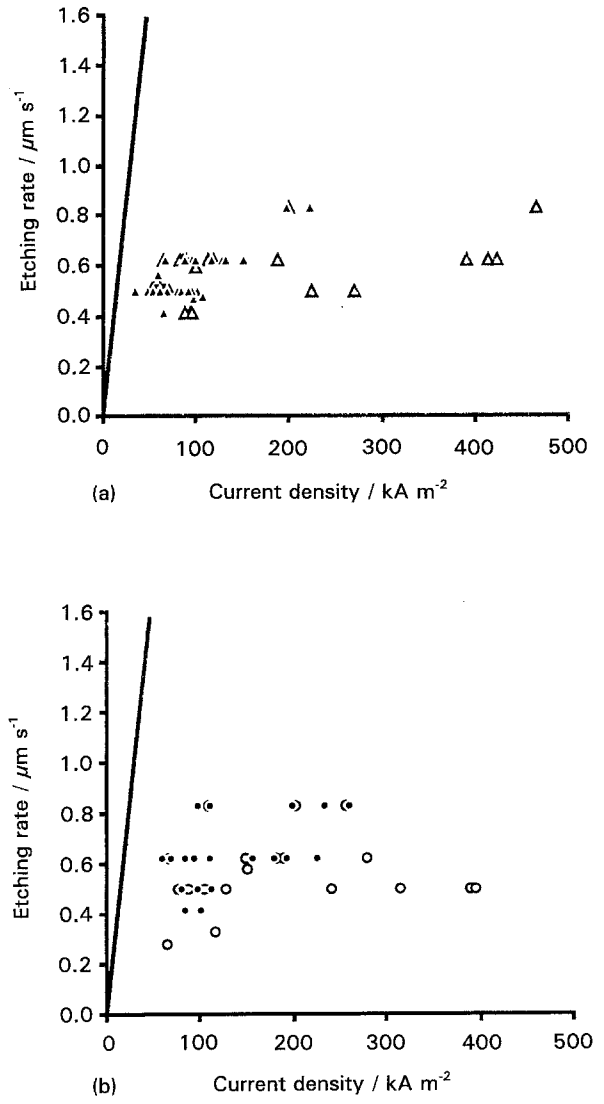

Fig. 4. Etching rates against the average current density; solid line refer to the theoretical etching rate. (a) Conical holes produced without (△) or with pulsed laser assistance (▲); (b) cylindrical holes produced without (○) or with pulsed laser assistance (●).

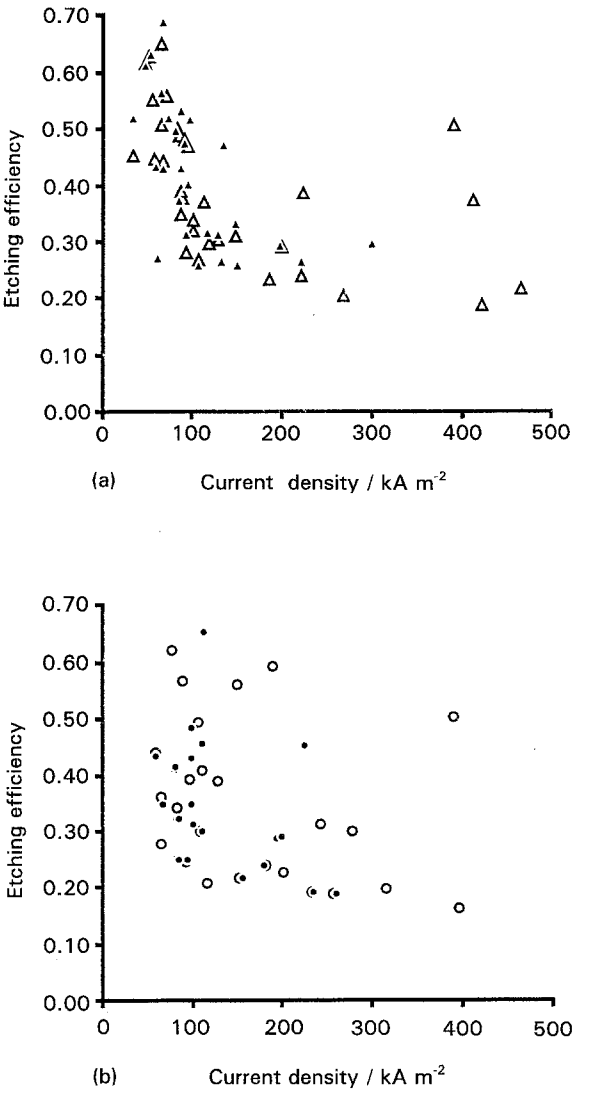

Fig. 5. Etching efficiency against the average current density. (a) Conical holes produced without (△) or with pulsed laser assistance (▲); cylindrical holes produced without (○) or with pulsed laser assistance (●).

the charge actually consumed:

$$\Phi = \frac{\nu_e F \rho V}{M \int_0^t I(t)\,\mathrm{d}t} \qquad (1)$$

where ρ is the specific gravity of the metal and M denotes its molecular weight. The deviation of this efficiency from unity expresses the significance of metal dissolution in the external zones. In spite of scatter of the experimental data, Fig. 5(a) and (b) shows that the etching efficiency is a decreasing function of the current density whatever the shape of the hole; Φ varies from 0.7 below 100 kA m^{-2} down to 0.20–0.30 for current densities over 400 kA m^{-2}. This means that etching on the peripheral zone and the ring zone is of greater significance for high current densities. The dispersion of data could not yield a definitive influence of the nozzle diameter on the efficiency; however it may be assumed that spreading phenomena are of higher significance with small nozzles and that the variations of Φ shown in Fig. 5 are due to flow phenomena at the metal surface. Moreover the assistance of the pulsed laser seems to have no influence on the etching efficiency.

3.4. *Shape of the hole and effect of the pulsed laser assistance*

The objective of the operation is hole drilling with the highest mechanical precision, the dimensions of the etched structure being as close as possible to the nozzle diameter. A shape factor was defined to compare the volume of the ideal hole (diameter d) to that of the hole actually machined in the nickel plate:

$$F_s = \frac{\pi d^2 e}{4V} \qquad (2)$$

Shape factors were calculated for holes exhibiting cylindrical geometry. For this case, F_s was simply reduced to the square of the ratio (d_r/d). The variations of this factor with the nozzle diameter and the current density were shown in Fig. 6(a) and (b). The effect of the pulsed laser beam on the shape factor is of minor significance. The shape factor

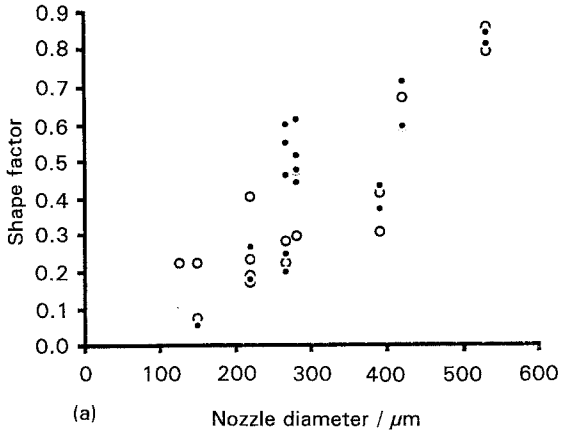

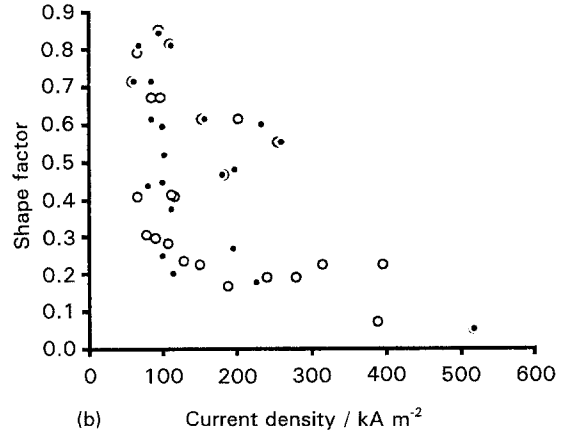

Fig. 6. (a) Shape factor against the nozzle diameter; experiments were conducted without (O) or with pulsed laser assistance (●). (b) Shape factor against the average current density; experiments were conducted without (O) or with pulsed laser assistance (●).

appears to vary linearly with nozzle diameter and to decrease regularly with current density. Using large nozzles with moderate current densities results in factors up to 90%: for these conditions, the diameter of the holes is fairly close to the nozzle diameter. Conversely, drilling with a 125 μm nozzle at 400 kA m^{-2} yields holes with a diameter near 280 μm.

The laser assistance was found to improve the mechanical precision of the etching operation: in particular, the edges of the holes were sharper and their profiles were more vertical and regular. When conducted with the incident laser beam, etching was confined to the impact zone, and the extent of the ring zone was reduced, in spite of unchanged values for the etching efficiency. This phenomenon can also be observed in Figs 7 and 8 related to the machining of pieces, described later. Pulsed laser irradiation results in a sudden rise in temperature during the energy pulse, followed by rapid quenching of the metal surface. As for zinc deposition [15], the thermal effect of the pulsed beam may improve the morphology of the hole wall and the mechanical precision.

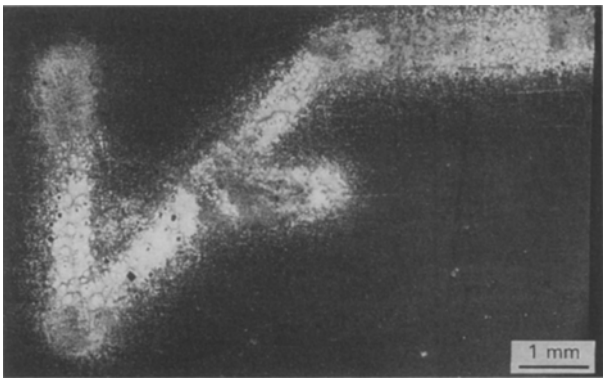

Fig. 7. Detail of an acronym etched continuously in a nickel plate using a 300 μm nozzle, without laser assistance; average current density: 72 kA m^{-2}.

4. Etching of small objects

The present device was applied to the etching of objects. First trials were carried out with the continuous displacement of the metal substrate. The low etching rates led to the adoption of a linear velocity below 100 μm s^{-1}. However, drastic overheating of the two step-by-step motors rendered this procedure unsuitable for times greater than a few minutes.

To overcome this, an alternative procedure was imagined. The pattern of the piece to be machined was divided into steps, the length of which were 20% lower than the nozzle diameter. The motion of the substrate was stopped during the hole drilling operation for a fixed period of 60 seconds; then the substrate was displaced to the following step and the drilling operation was repeated. In this case, the step-by-step displacement could be performed with velocities large enough to avoid any damage of the motors. In addition, the time of motionless dissolution was chosen to allow the complete drilling of each successive hole.

Two pieces were machined using the step-by-step technique, namely on acronym (12 mm × 7 mm) and a star (diam. 5 mm), with or without laser assistance, and using an Altuglas/silicon nozzle of 125 μm × 125 μm and an Altuglas nozzle of 219 μm. For all experiments presented, the applied voltage was 40 V. Due to the step length, compared with

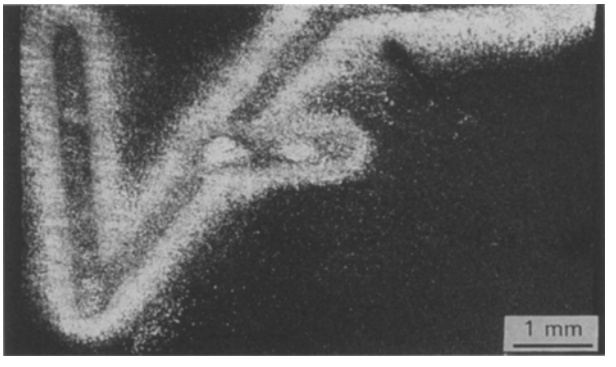

Fig. 8. Detail of an acronym etched continuously in a nickel plate using a 300 μm nozzle, with laser assistance; average current density: 87 kA m^{-2}.

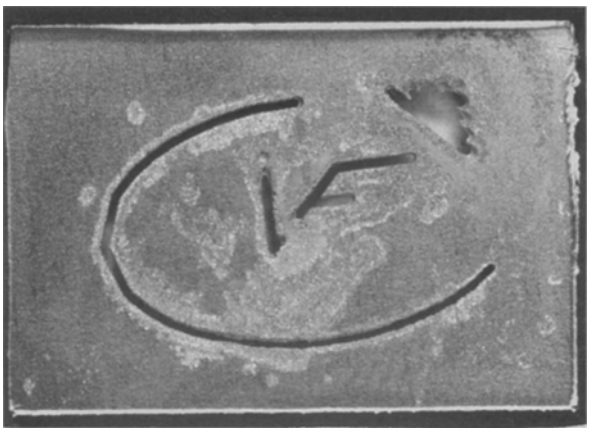

Fig. 9. Example of an acronym etched using a 219 μm nozzle; step length: 170 μm; without laser assistance; average current density: 117 kA m^{-2}.

Fig. 10. Example of an acronym etched using a 219 μm nozzle; step length: 170 μm; with laser assistance; average current density: 146 kA m^{-2}.

the nozzle diameter, the cylindrical shapes of the individual holes were not visible and the profiles of the pieces were quite regular.

Taking into account the period of motionless drilling, the step length and the nickel sheet thickness, the etching rate could be estimated to be 2 μm s^{-1}. This is far higher than the value obtained for single-hole drilling, possibly due to the very different operating conditions, since etching of a surface corroded during the preceding drilling operation, is easier than dissolution of a perfect plane surface.

For the larger nozzle (219 μm), a significant effect of the laser beam can be observed in Figs 10 and 12 to be compared with Figs 9 and 11, respectively: under irradiation, the dissolution is more confined, the edges are sharper and the walls perfectly vertical. The average width of the etched piece is reduced from 350 to 275 μm with laser assistance. In agreement with the observations made above, the use of small nozzles seems to be less promising: the etching appears to be less regular and the line width, near 250 μm, is not significantly modified by the laser assistance. This was attributed to a different flow regime of the jet for the smaller nozzle. In this case, the spreading of liquid on the vertical plate is more significant; this reduces the precision of the jet etching and hinders the effect of the pulsed laser beam.

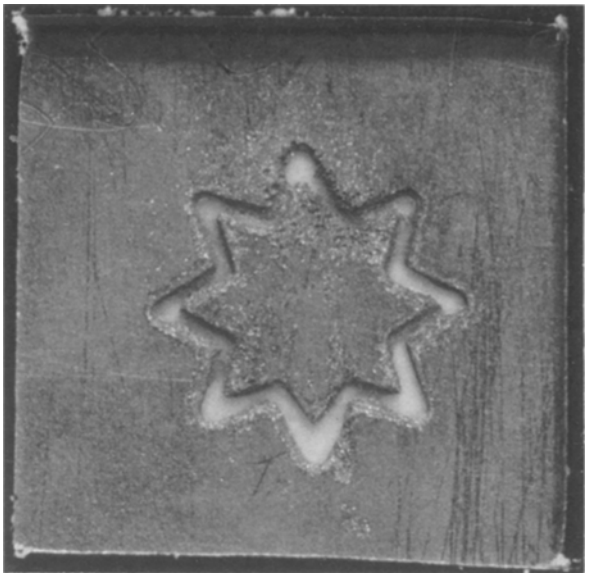

Fig. 11. Machining a star out of a nickel sheet using a 219 μm nozzle; step length: 170 μm; without laser assistance; average current density: 394 kA m^{-2}.

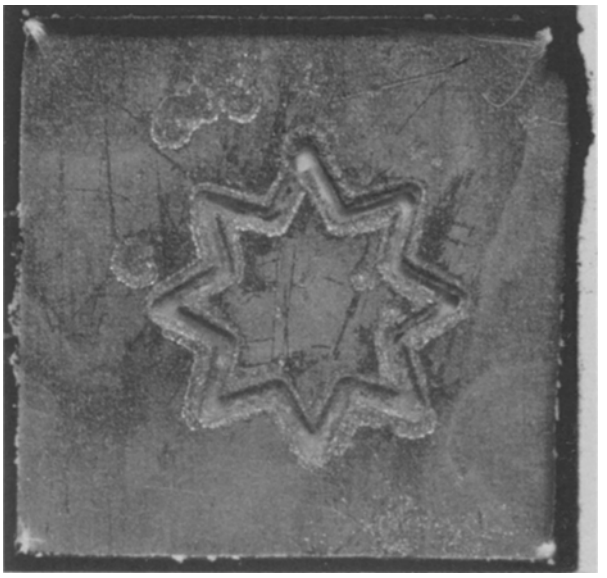

Fig. 12. Machining a star out of a nickel sheet using a 219 μm nozzle; step length: 170 μm; with laser assistance; average current density: 419 kA m^{-2}.

Acknowledgements

The authors thank Drs D. Hauden and S. Ballandras of the Laboratoire de Physique et Métrologie des Oscillateurs, Besançon, France, for their kind assistance in manufacturing the silicon pieces.

References

[1] M. Datta and L. T. Romankiw, *J. Electrochem. Soc.* **136** (1989) 285C.
[2] M. Datta and D. Landolt, *Electrochimica Acta* **25** (1980) 1255. See also *ibid.*, p. 1263.
[3] C. Van Osenbruggen and C. De Regt, *Philips Technical Revue* (1974).

[4] E. W. Becker, W. Ehrfeld and D. Münchmeyer, *Microelectron. Eng.* **4** (1986) 35.
[5] C. Burbaum, J. Mohr, P. Bley and W. Menz, *Sensors and Materials* **3** (1992) 075.
[6] B. J. Sedon, Y. Shao, J. Fost and H. H. Girault, *Electrochim. Acta* **39** (1994) 783.
[7] J. A. McGeough, 'Principles of electrochemical machining', Wiley & Sons, New York (1974).
[8] L. W. Hourng and C. S. Chang, *J. Appl. Electrochem.* **24** (1990) 1170.
[9] T. H. Drake and J. A. McGeough, Proceedings of Machine Tool Design and Research Conference, Manchester, UK, Macmillan, London (1981) p. 361.
[10] B. Sajdl and I. Rousar, *J. Appl. Electrochem.* **24** (1994) 883.
[11] M. R. C. Bocking, Proceeding of the 1st European Conference of Rapid Prototyping, University of Nottingham, UK, 6–7 July (1992) p. 95.
[12] R. J. von Gutfeld, *J. Opt. Soc. (USA), B*, **4**(2) (1987) 272.
[13] M. H. Gelchinski, D. R. Vigliotti and L. T. Romankiw, *J. Electrochem. Soc.* **132** (1985) 2575.
[14] M. Datta, L. T. Romankiw, D. R. Vigliotti and R. J. von Gutfeld, *ibid.* **136** (1989) 2251.
[15] I. Zouari, F. Lapicque, M. Calvo and M. Cabrera, *ibid.* **139** (1992) 2163.
[16] I. Zouari, C. Pierre, M. Calvo and F. Lapicque, *J. Appl. Electrochem.* **23** (1993) 863.
[17] J. T. Davies, 'Turbulence phenomena', Academic Press, New York (1972).